Copy 5
RM L57G23

NACA

RESEARCH MEMORANDUM

ANALOG COMPUTER STUDY OF SOME FILTERING, COMMAND-COMPUTER, AND AUTOMATIC-PILOT PROBLEMS CONNECTED WITH THE ATTACK PHASE OF THE AUTOMATICALLY CONTROLLED SUPERSONIC INTERCEPTOR

By Windsor L. Sherman

Langley Aeronautical Laboratory
Langley Field, Va.

CLASSIFIED DOCUMENT

NATIONAL ADVISORY COMMITTEE
FOR AERONAUTICS

WASHINGTON

October 3, 1957

CONFIDENTIAL

NACA RM L57G23

NATIONAL ADVISORY COMMITTEE FOR AERONAUTICS

RESEARCH MEMORANDUM

ANALOG COMPUTER STUDY OF SOME FILTERING, COMMAND-COMPUTER, AND AUTOMATIC-PILOT PROBLEMS CONNECTED WITH THE ATTACK PHASE OF THE AUTOMATICALLY CONTROLLED SUPERSONIC INTERCEPTOR

By Windsor L. Sherman

SUMMARY

Presented herein are the results of a study of some of the problems associated with the cross-roll filter, command computer, and g-limiter of an automatic interceptor system. The evaluation of these components was made with straight-flying targets and targets that made a ±2g vertical-plane maneuver. The interceptor system used assumes lead-collision fire-control computing and an armament of unguided rockets. This interceptor system is described in NACA RM L56J08.

The results, which are presented as time histories of the airplane and control-surface motions, show that cross-roll corrections are most desirable when filtering in a rotating coordinate system and that, when an inner-loop integrator is included in the longitudinal control system, the best operation of the command type of g-limiter is obtained. In addition, the results for the command computer show that although the present computer provided adequate control for this study, more study is needed on the problem of roll-command computation. Also, the results for the maneuvering target indicate that a high-gain longitudinal control system is necessary when tracking a maneuvering target.

INTRODUCTION

One means of defense against strategic bombers is the manned interceptor. At present these interceptors are equipped with fire-control apparatus but must, in general, be flown by a pilot. The projected development of this type of weapons system is to make the attack phase of the interceptor completely automatic. This phase begins with the

airborne intercept radar lock on and ends with the firing of the interceptor armament. Reference 1 is a report of an investigation of the flight maneuvers of an interceptor during the attack phase and of the manner in which the response of the interceptor was affected by nonlinear aerodynamics and changes in the dynamic representation of the interceptor.

In addition to the airplane and fire-control equipment, an automatic interceptor system has an error filter system, a command computer, and an automatic pilot. The method of filtering and computing and the choice of gains in these three components can and do influence the response of the interceptor. The purpose of the investigation reported herein was to study the effects of certain changes in computing and gains on the response of the interceptor described in reference 1. For this purpose the effects of cross-roll corrections in the filter system, changes in the roll-command computing, the command g-limiter, and gain changes in the longitudinal control system were studied. This study was conducted concurrently with the investigation reported in reference 1 on the typhoon computer at the U. S. Naval Air Development Center, Johnsville, Pa.

In this study the assumption was made that a Mach number 2.2 interceptor executed a forward-hemisphere attack against a Mach number 1.4 target that was flying a straight-line course or making a ±2g vertical-plane maneuver that started at radar lock on. Results are presented in the form of time histories obtained from an analog computer. The results illustrate the effects of the aforementioned changes. Representative results are included to show the effectiveness of the airplane-autopilot combination against the maneuvering target. All results presented in this paper were obtained under the basic assumption that the interceptor armament consisted of unguided rockets.

SYMBOLS

u,v,w	linear airplane velocities along the x,y,z body axes, ft/sec
p,q,r	angular airplane velocities about the x,y,z body axes, radians/sec
g	acceleration of gravity, 32.18 ft/sec^2
n	normal acceleration
M	Mach number, $\frac{V}{a}$
$\bar{c}$	mean aerodynamic chord
$\overrightarrow{V_m}$	missile velocity vector with respect to airplane, ft/sec

$\vec{V_F}$	airplane velocity vector, $\left\|V_I\right\| = \sqrt{u^2 + v^2 + w^2}$, ft/sec
$\vec{V_T}$	target velocity vector, ft/sec
a	free-stream velocity of sound, ft/sec
$\vec{a_T}$	target acceleration vector, ft/sec^2
M_a	azimuth miss distance, ft
M_e	elevation miss distance, ft
$\vec{R}$	range vector, ft
R_f	future range
$\vec{M}$	total vector miss distance ($M = \vec{i}(0) + \vec{j}M_a + \vec{k}M_e$), ft
E_a, E_e	unsmoothed azimuth and elevation steering errors
t	time
t_g	time to go, sec
$D = \frac{d}{dt}$	
s	Laplace transform variable
n_z	direction cosine between airplane and space vertical axes
C_l	rolling-moment coefficient
C_m	pitching-moment coefficient
C_n	yawing-moment coefficient
C_Z	lift coefficient in body axes
H_T	altitude, ft
H(s)	transfer function $\dot{\gamma}/\delta_e$ of airplane
$\dot{\gamma}$	flight-path angular rate ($\dot{\theta} - \dot{\alpha}$)
F(s)	transfer function q/δ_e of airplane

$K_1, K_2, \ldots$	gain constants
ϵ	total smoothed steering error $\left(\epsilon = \epsilon_a^2 + \epsilon_e^2\right)$
ϵ_a	smoothed azimuth steering error, radians
ϵ_e	smoothed elevation steering error, radians
θ	Euler angle and airplane pitch angle
δ	control-surface deflection, deg
$\vec{\omega_D}$	angular velocity vector of line of sight of radar, $(\vec{\omega} = \vec{i}p + \vec{j}q + \vec{k}r)$, radians/sec
$\vec{i}, \vec{j}, \vec{k}$	unit vectors
τ	time of missile flight, sec; or control-system time constant, sec
ϕ	bank angle
β	sideslip angle $\left(\beta \approx \frac{v}{V}\right)$, radians
δ_r	rudder deflection
δ_a	aileron deflection
α	angle of attack $\left(\alpha \approx \frac{w}{u}\right)$, radians
S	wing area
θ_a, θ_e	azimuth and elevation gimbal angles, radians
ψ	Euler angle and airplane yaw angle
Δ	with another symbol, indicates perturbation of attached symbol

$$C_{m_q} = \frac{\partial C_m}{\partial\left(\frac{qc}{2V}\right)}$$

$$C_{Z_\alpha} = \frac{\partial C_Z}{\partial \alpha}$$

$$C_{m_\alpha} = \frac{\partial C_m}{\partial \alpha}$$

$$C_{m_{\delta_e}} = \frac{\partial C_m}{\partial \delta_e}$$

$$C_{Z_{\delta_e}} = \frac{\partial C_Z}{\partial \delta_e}$$

A dot over a symbol denotes the derivative with respect to time.

Subscripts:

o	indicates initial condition or output
cr	critical
c	command
d	dynamic pressure
e	limit value of variable
f	filter time constant
i	input
l	limit
ss	steady state

SIMULATION AND DESCRIPTION OF THE CONTROL SYSTEM

The analog setup for the Typhoon Computer which was used in this study is described fully in reference 1.

Figure 1 is a block diagram of the flight-control system, the portion of the interceptor system considered in detail in this report. As indicated in figure 1, an error filter system, a command computer, an autopilot, and an airplane are considered. The filter system consists of two first-order filters, one for the lateral command and one for the longitudinal command, with a roll multiplier for cross-roll correction. The command computer consists of a g-limiter, and a roll-order computer. Manually adjustable gains K_3 and K_4 are applied to the output of the roll-command computer and g-limiter before these outputs are fed to the automatic pilot.

The automatic pilot provided proportional type control and had rate and acceleration feedbacks in the roll-control and flight-path-control loops, while the rudder is controlled by a yawing velocity or sideslip angular-rate feedback. The servomotors in the autopilot were represented by first-order equations, with rate and displacement limiting added to the simulation. These autopilots were analyzed on the analog computing equipment at the Langley laboratory to determine their suitability for use in this study. The results of these studies are reported in references 2 and 3.

The interceptor used was a high-speed airplane of advanced design. The basic aerodynamics were calculated by the use of linear theory, and the results are given in reference 4. These data were then modified, as indicated in reference 1, so that the nonlinear variations of the aerodynamic forces and moments with angle of attack were accounted for in the simulation. Drag data and control-surface effectiveness were obtained from wind-tunnel tests. In this study the airplane was always represented by the six-degree-of-freedom equations of rigid-body motion referred to principal body axes. The same sets of initial conditions were used for the current study as were used in the study reported in reference 1. For convenience, these conditions are repeated in table I and figure 2.

The table of initial conditions contains no initial values for $\vec{\omega}_D$, $\vec{M}$, $\vec{R}_f$, ϵ_a, ϵ_e, and ϕ_c. The initial value of each of these parameters is automatically determined if the values from table I are substituted in the equations of the interceptor system which are presented in appendix A of reference 1.

In these attack runs it was assumed that the radar had been tracking the target long enough so that the fire-control computer had completely charged the filters before commands were fed to the autopilot. Because of this assumption the following initial conditions were imposed upon the error filter system.

$$\epsilon_a(0) = E_a(0) \qquad \dot{\epsilon}_a(0) = 0 \qquad \epsilon_e(0) = E_e(0) \qquad \dot{\epsilon}_e(0) = 0$$

In addition, the servomotors for the autopilot were programmed with the following initial condition.

$$\delta_o(0) = 0 \qquad \dot{\delta}_o = \frac{\delta_i(0)}{\tau_s}$$

RESULTS AND DISCUSSION

The Cross-Roll Filter

Because a tracking radar output consists of a true signal plus some random-noise signal and because of the dynamics of the computers, the information signals must be smoothed before they are combined and used as steering signals for the airplane. This smoothing or filtering may be applied to either the target velocity, which under the assumptions of a first-order fire-control system is essentially time invariant, or to the output of the fire-control computer. In the system considered in this report, the filtering is applied to the output of the fire-control computer which is essentially the lead-angle error. The computer output is the vector error $\vec{E}$, and

$$\vec{E} = \vec{i}(0) + \vec{j}E_a - \vec{k}E_e \tag{1}$$

which is a two-component vector. There is no i component as this component was driven to zero in obtaining a solution of the fire-control equations. In this interceptor system $\vec{E}$ is smoothed by a first-order filter. This filter is represented by the equation

$$\vec{E} = \vec{\epsilon} + \tau_f D\vec{\epsilon} \tag{2}$$

where $\vec{\epsilon}$ is the smoothed value of $\vec{E}$ and $\vec{\epsilon} = \vec{i}(0) + \vec{j}\epsilon_a - \vec{k}\epsilon_e$. If the filtering takes place in inertial coordinates, equation (2) provides a correct $\vec{\epsilon}$; however, if the axis system is rotating, $\vec{\epsilon}$ is dependent upon the angular rate and position of the coordinate system in which the filtering takes place. If the total derivative of $\vec{\epsilon}$ is taken with respect to inertial space and the corresponding terms are fed back to the input of the filter, the dependence upon the angular motion of the coordinate system is eliminated. Thus the filter equation becomes

$$\vec{E} = \vec{\epsilon} + \tau_f\left[\frac{d}{dt}(\vec{\epsilon}) + \vec{\omega}_A \times \vec{\epsilon}\right] \tag{3}$$

where $\vec{\omega}_A$ is the angular-velocity vector of the interceptor. Equation (3) represents a filter that corrects for angular velocity but still filters the linear motions of the interceptor. In this former respect, this filter is similar to the vector filter proposed in reference 5. Under the assumption that $\vec{\epsilon}$ is a two-component vector, the filter equations used in this study are as follows:

$$\left.\begin{aligned} E_a &= \epsilon_a + \tau_f\left(\dot{\epsilon}_a + p\epsilon_e\right) \\ E_e &= \epsilon_e + \tau_f\left(\dot{\epsilon}_e - p\epsilon_a\right) \end{aligned}\right\} \tag{4}$$

The assumption of a two-component $\vec{\epsilon}$ eliminates the q and r corrections in ϵ_a and ϵ_e. In addition, this filter neglects a correction term $\left(-q\epsilon_e - r\epsilon_a\right)$ which could conceivably affect the assumption of a zero i component of $\vec{\epsilon}$. Since q and r are small, and in this investigation were of opposite sign during the critical phase of the attack run, the error introduced by the neglect of these terms is thought to be negligible.

In order to illustrate the effect of the rolling corrections in the cross-roll filter, equations (2) and (4) were used to calculate the response of a simple filter and of a filter in which the cross-roll correction was used. It was assumed that an error fixed in space was viewed from a steadily rolling interceptor; thus,

$$\vec{E}(t) = \vec{i}(0) + \vec{j}E_a(t) - \vec{k}E_e(t)$$

where the elevation and azimuth components of the error are given by $E_e(t) = E_{e_o} \cos pt$ and $E_{a_o}(t) = -E_{e_o} \sin pt$ because of the rolling velocity of the interceptor. In addition, it was assumed that the filter was initially charged, which gave $\epsilon_{e_o}(0) = E_{e_o}(0)$ and $\epsilon_{a_o}(0) = E_{a_o}(0) = 0$. When these inputs and initial conditions are used, the solution for elevation channel of the simple filter is

$$\epsilon_e(t) = E_{e_o}\left(1 - \frac{1}{1 + \tau_f{}^2p^2}\right)e^{-t/\tau_f} + \frac{E_{e_o}}{\left(1 + \tau_f{}^2p^2\right)^{1/2}} \cos(pt - \theta) \tag{5}$$

where $\theta = \tan^{-1}(\tau p)$. This equation clearly shows the dependence of $\epsilon_e(t)$ on the interceptor rolling velocity and filter time constant. When the cross-roll correction is included in equation (4), the solution for $\epsilon_e(t)$ is

$$\epsilon_e(t) = E_{e_o} \cos pt \tag{6}$$

which is the unmodified input of the filter. This solution is obtained under the assumption of an initially charged filter where the transient solution goes to zero and leaves only the steady-state solution.

For purposes of comparing these solutions, equations (5) and (6) have been plotted in figure 3 for a unit E_e and a value of p of 2.5 radians per second. These results show that the output of the simple filter is attenuated and lags the input by the angle θ; whereas, when the cross-roll correction is included, the output of the filter system is the same as the input. The attenuation and phase lag of the output of the simple filter are caused by the smoothing of the changes in E_e that are due to motion of the interceptor. The cross-roll correction applied in the cross-roll filter compensates for the changes in E_e due to interceptor motion and thus eliminates the attenuation and phase lag.

Figure 4 presents the effect of omitting the cross-roll correction in the filter on the response of the interceptor. The main effect of the cross-roll correction is to smooth the oscillations that occur in the airplane response. This smoothing may be of importance in the roll response as it is the roll response that determines the magnitude of the sidewise acceleration impact on the pilot's head during the maneuver. The data obtained in this study did not indicate a significant difference in the predicted terminal miss distances when the cross-roll correction was omitted.

The Command Computer

The function of the command computer is to convert the filtered steering errors (ϵ_a and ϵ_e) to automatic-pilot commands. As ϵ_e represents a flight-path error, no further modification of this quantity was necessary, and the value of the error was passed on to the g-limiter and automatic pilot. In the case of the roll command, it was desired to command a roll rate that varied directly with the magnitude of the bank-angle error. The desired change in bank angle ϕ_c was defined by the equation

$$\phi_c = \tan^{-1} \frac{\epsilon_a}{\epsilon_e} \tag{7}$$

which neglects the effect of gravity on the magnitude of the bank angle. One result of omitting gravity considerations is the introduction of large roll orders for a finite ϵ_a as $\epsilon_e \rightarrow 0$. When the low-gain flight-path-control system of reference 1 was used to control the longitudinal motion of the airplane, satisfactory roll control was obtained (see fig. 5). As shown in figure 5, however, substitution of the high-gain flight-path-control system caused unsatisfactory roll response. The time history of $\frac{M_e}{t_g + \tau}$ for the high-gain flight-path-control systems changes sign several times while that for the low-gain flight-path-control system does not change sign. As ϵ_e is the smoothed value of E_e, which by definition

is $\frac{\frac{M_e}{t_g + \tau}}{V_F + \frac{V_m}{t_g + \tau}}$, changes in the sign of $\frac{M_e}{t_g + \tau}$ generally produce corresponding changes in sign in ϵ_e. These sign changes in ϵ_e are the cause of the violent rolling motions shown in figure 5.

Three modifications of the arc tangent roll-command computation were studied to determine if the large rolling motions could be eliminated. Figure 6, which presents a sketch of the command-computer output, is used in the discussion of these modifications. The axes of the computer are coincident with the reference axes of the interceptor, and the predicted impact point may appear in any one of the four quadrants. The predicted impact point is displaced from the origin by the steering errors ϵ_a (along the Y axis) and ϵ_e (positive along the negative Z axis of the interceptor). The circle centered at the origin with a radius of ϵ_{cr} is called the ϵ_{cr} boundary. The value of ϵ_{cr} is a predetermined value of ϵ which is the total steering error and is defined as $\epsilon = \sqrt{\epsilon_a^2 + \epsilon_e^2}$. As the interceptor maneuvers to reduce the steering errors to zero, the predicted impact point and the origin, which represents the rocket line of the interceptor move towards each other. When $\epsilon = \sqrt{\epsilon_a^2 + \epsilon_e^2} \leq \epsilon_{cr}$, the predicted impact point appears within the ϵ_{cr} boundary.

The first modification of the roll command used the dead-zone concept, and no-roll control was provided within the ϵ_{cr} boundary. The value of ϵ_{cr} was based on the maximum acceptable miss distance for a kill which gave an ϵ_{cr} of about 0.01667. This method proved completely unsatisfactory because the interceptor did not fly so as to hold the steering error within the ϵ_{cr} boundary. Very erratic motions occurred whenever the ϵ_{cr} boundary was crossed. In the second modification of the roll command, the computation was changed from $\phi_c = \tan^{-1}\frac{\epsilon_a}{\epsilon_e}$ to $\phi_c = K\epsilon_a$ inside the ϵ_{cr} boundary. This modification gives control proportional to the azimuth steering error. Several runs were made to determine a reasonable value of K and the size of the proportional control zone. It was found that values of $K = 16$ and $\epsilon_{cr} = 0.03$ provided good but not optimum control. As shown in figure 7, this modified roll command considerably decreased the very large rolling velocities that occur when ϵ_e passes through zero; however, the interceptor did not fly so as to hold the steering error within the proportional control zone, and relatively large rolling velocities still developed when the ϵ_{cr} boundary was crossed. The frequency of the crossings was much less

than in the first modification. The third and final modification of the roll-command computer introduced the concept of small bank-angle selection, that is, the selection of the smallest of the two possible bank angles that exist for a given situation, in the proportional control zone. If the steering error dot appears in the fourth quadrant of figure 6, the interceptor can roll to the right through a bank angle greater than 90° or roll left through a small bank angle and use negative normal acceleration to close on the target. The third modification is the same as the second except that when ϵ_e is negative the bank-angle command ϕ_c is multiplied by -1. It should be noted that this modification (the multiplication by -1) occurs only within the ϵ_{cr} boundary. As the roll control is proportional to the azimuth steering error in this region, the negative of the true azimuth steering error will cause the airplane to roll through the smallest bank angle and push down on the target. This third modification of the roll command caused the interceptor to fly so that the steering error was held within the proportional control zone. As shown in figure 7, the amplitude of the rolling motions in the last part of the attack run has been considerably reduced, when compared to those obtained with the other roll commands, and a smoother ride for the pilot is obtained. It is interesting to note that with this last roll-command modification, the smallest predicted terminal miss distances were obtained. It should be noted that this decrease in the miss distance was not significant in determining the success or failure of the attack run.

The use of the small bank angle introduced a new problem. Whenever the interceptor rolled to the smallest bank angle, it rolled and sideslipped in such a manner that it assumed an inverted position below the target and completed the run by pulling up with negative normal acceleration. This condition, which may have been caused by the omission of gravity considerations in the roll-command computation, is illustrated by the time histories of normal acceleration and the direction cosine n_z shown in figure 8.

The g-limiter

A g-limiter was used in this study to restrict the normal acceleration of the interceptor to realistic values. No attempt was made to study the overall g-limiting problem; however, during the course of this investigation some rather interesting information was obtained on g-limiting.

Some preliminary simulator flights were made with a feedback type of g-limiter. With this type of limiter, the normal acceleration of the airplane was measured and when it exceeded a predetermined value, in this case 5g or -2g, a signal was fed directly to the elevator servo to reduce the normal acceleration. Because the normal acceleration had to develop before the limiter could restrict it, large overshooting developed due to the time lag between the action of the elevator and the change in normal acceleration.

As shown in figure 1, the command g-limiter operates on the incoming command so that the commanded steady-state normal acceleration never exceeds the desired value. As the characteristics of the airplane and automatic pilot influence the setting of the g-limiter, a linear analysis was made for longitudinal control systems with and without inner-loop integrators to determine the important parameters for the g-limiter setting. The transfer function for $\dot{\gamma}/\epsilon_e$ of this control system (see fig. 1) is

$$\frac{\dot{\gamma}}{\epsilon_e} = \frac{K_4\left(\frac{K_8}{s} + K_6\right)H(s)}{1 + \tau s + \left(K_{12} + K_{20}s\right)F(s) + \left(\frac{K_8}{s} + K_6\right)H(s)} \tag{8}$$

where $F(s)$ and $H(s)$ are the airplane transfer functions q/δ_e and $\dot{\gamma}/\delta_e$, respectively, based on a representation of the motion of the airplane by the pitching-moment and normal-force equations. The two cases that were considered corresponded to an inner-loop integrator included ($K_8 \neq 0$) and the inner-loop integrator deleted from the control system ($K_8 = 0$). The steady-state $\dot{\gamma}/\epsilon_e$ for a step input of ϵ_e is obtained from equation (8) by letting s approach zero. Thus, for $K_8 \neq 0$

$$(\dot{\gamma}/\epsilon_e)_{ss} = K_4 \tag{9}$$

and for $K_8 = 0$

$$(\dot{\gamma}/\epsilon_e)_{ss} = \frac{K_4 K_6}{C + K_6 + K_{12}} \tag{10}$$

where C is a constant, and

$$C = \frac{\left(C_{m_q} C_{Z_\alpha} qS\bar{c} - 2mV^2 C_{m_\alpha}\right)}{2Vq_d S\left(C_{Z_\alpha} C_{m_{\delta_e}} + C_{Z_{\delta_e}} C_{m_\alpha}\right)} \tag{11}$$

The above steady-state expressions were used to determine g-limiter settings. When the integrator was included, ($K_8 \neq 0$), the g-limiter setting is given by

$$\epsilon_{e_l} = \frac{n_l g}{V}\frac{1}{K_4} \tag{12}$$

and when the integrator was deleted ($K_8 = 0$), by

$$\epsilon_{e_l} = \frac{n_l g}{V} \frac{K_6 + K_{12} + C}{K_4 K_6} \tag{13}$$

Equations (12) and (13) show that the airplane and autopilot characteristics do not influence the setting of the g-limiter when the inner-loop integrator is included in the control system but that the airplane automatic-pilot characteristics must be accounted for in the g-limiter setting when the inner-loop integrator is omitted from the longitudinal-control system.

Figure 9 shows the normal acceleration response of the control system with the inner-loop integrator included in the control system. Figure 9(a) shows the limited and unlimited normal-acceleration responses for initial condition III with a linear pitching moment. As can be seen, the unlimited case is completely unsatisfactory; whereas, the limited case remains below the 5g limit. Figure 9(b) shows the same responses when the pitching moment is nonlinear. Again the unlimited response is much too high to be satisfactory. With the g-limiter in operation, the normal acceleration has a maximum overshoot of about 0.5g, but the average normal acceleration is about 5g. Figure 10 shows the case where the inner-loop integrator is omitted from the control system. When the pitching moment was linear the maximum overshoot was about 1.4g, and when the pitching moment was nonlinear, the maximum overshoot was about 2.8g. No runs for unlimited acceleration are usable for these cases as a severe limiting condition rendered the results questionable. The extreme overshoots in the case of the nonlinear pitching moment were probably caused by the fact that C_{m_α} was assumed to be constant in determining the g-limiter setting but C_m was varied as a function of angle of attack and Mach number in the pitching-moment equation. The g-limiter response, when the inner-loop integrator is omitted, is considered unsatisfactory, even though the average normal acceleration is about 5g with a linear pitching moment, because of the magnitudes of the initial overshoots which could severely overload an airplane.

It should be noted that the automatic-pilot gains were different for the two cases considered; however, this difference in gain does not affect the results as far as the integrator is concerned because the same value of the gains was used in the automatic-pilot setting and in the g-limiter setting.

The Maneuvering Target

In order to understand the problems involved in developing a control system for an interceptor tracking a maneuvering target, it is necessary

to understand how the orders supplied to the control system are obtained. The vector equation

$$\vec{R} + \vec{V_T}(t_g + \tau) - \vec{V_F}(t_g + \tau) - \vec{V_m}\tau = \vec{M} \qquad (14)$$

presents a first-order simulation of the miss-distance prediction for lead-collision fire control. When the target velocity remains unchanged $\left(\vec{a_T} \text{ is zero}\right)$, this equation provides an accurate solution of the fire-control problem. If the target develops an acceleration, this equation no longer gives an accurate solution as there are no acceleration terms included in the prediction; however, there is an effect on the prediction due to the history of target motion. As the target velocity vector $\vec{V_T}$ changes under the influence of the target acceleration, different miss-distances are predicted which cause the interceptor to change from steady to accelerated flight. Equation (14) shows, and analog studies substantiate, that the interceptor develops an acceleration approximately proportional to that of the target; however, in order to develop and hold this acceleration, for the formulation of the fire-control problem presented in equation (14), a steady-state error must exist. In addition to this steady-state error, an additional error is introduced which arises because the target is accelerating while the rocket is traveling from the firing point to the impact point predicted at the instant of firing $(t_g = 0)$.

It is most natural to consider the addition of acceleration terms to first-order computer as a solution to this problem. Unfortunately, acceleration terms are hard to obtain from the airborne intercept radar, and to date little success has been attained with second-order computers, primarily because of the noise associated with acceleration information.

There are two other methods available for reducing the steady-state tracking error. One method is to introduce a tracking integrator which adds an integral of the steering error to the input of the g-limiter. The second method is to increase the forward-loop gain, n/ϵ_e, of the longitudinal control system. Simply stated, this latter method means that the amount of normal acceleration ordered per degree of steering error is increased. Neither of these methods affects the error introduced by target acceleration during the time of flight of the rocket. Unless second-order computing is used, this is an error that must be tolerated; however, it can be kept small by using short times of rocket flight. Both of these methods are discussed in reference 6 for the vertical-plane problem. As shown in reference 6, the tracking integrator reduces the steady-state tracking error to zero when optimumized for a specific case; however, the results of reference 6 appear to indicate that the tracking-integrator gain should be a nonlinear function of steering error or miss

distance for the tracking integrator to function equally well for all conditions. The problem of a nonlinear gain is thus introduced. The second method, which increases the n/ϵ_e of the airplane-autopilot combination, does not eliminate the steady-state tracking error but reduces this error to acceptable magnitudes. This condition occurs because some error is needed in order to cause the interceptor to maintain normal acceleration to track the target. Generally speaking, control-system stability considerations will dictate the maximum forward-loop gain that can be used which, in turn, will determine the tracking error.

In order to avoid the complexity of a nonlinear gain, a high-gain longitudinal control system was used in tracking runs against the maneuvering target. The forward-loop gain of this control system was adjusted so that a value of n/ϵ_e of 1.4 was obtained for the airplane-autopilot combination.

In order to obtain some idea of the errors that occur when a control system found satisfactory against nonmaneuvering targets is used to track a maneuvering target, tracking runs were made against a maneuvering target with the two longitudinal control systems used in this study. Time histories of the interceptor tracking a nonmaneuvering target using these longitudinal control systems, a low-gain one and a high-gain one, are presented in reference 1.

Figure 11 compares the tracking ability for the low-gain and high-gain longitudinal control systems when the target was making a 2g pull-up. The low-gain control which has a value of n/ϵ_e of 0.4 gives a miss distance of approximately 403 feet, and the high-gain control system which has a value of n/ϵ_e of 1.4 gives a miss distance of about 115 feet which, for purposes of this study, was considered to be an acceptable miss distance.

The use of a high-gain control system and a command g-limiter present an interesting problem in system requirements. The use of an inner-loop integrator with the command type of g-limiter is most desirable as it is an important factor in obtaining an accurate normal acceleration restriction; however, when the forward-loop gain is increased to obtain good tracking of a maneuvering target, the presence of the integrator introduces an oscillation which has a period of approximately 30 seconds and damps to one-half amplitude in about 34 seconds. The removal of the integrator eliminates this oscillation. The problem presented is that of obtaining a compromise which provides enough integration to give acceptable g-limiting and at the same time introduces no unacceptable oscillations when a high forward-loop gain is used. As would be expected, the combination of high gain and the continuous demand for normal acceleration resulting from the maneuver of the target produced a most undesirable rate limiting condition in $\dot{\delta}_e$. The use of the nonlinear pitching moment in the airplane representation aggravated the rate limiting condi-

tion and increased the roughness of the ride. A pitching-acceleration feedback loop was added to the control system in an attempt to alleviate the rate limiting condition. Figure 12 shows the effect of a pitching-acceleration feedback with a gain of 0.1 when a nonlinear pitching moment was used. The inclusion of this feedback completely eliminates the rate-limiting oscillation in the control-surface motion. The control of this oscillation smooths the response of the airplane. Figure 12 also indicates that the rate-limiting oscillation does not affect the ability of the interceptor system to reduce the elevation steering errors.

The study also included the case of a target performing a 2g push-down maneuver. As the interceptor normally starts below the target, the interceptor starts to pull up towards the predicted interception point. In the case of target pull-up, the interceptor keeps pulling up; however, when the target executes a push-down maneuver, the downward motion of the target and the upward motion of the interceptor cause the predicted impact point to appear below the flight path of the interceptor. The interceptor must, therefore, reverse its direction either by rolling to pull down on the predicted impact point or by rolling through a small angle and pushing down. It was anticipated that this change in direction might cause deterioration of the interceptor tracking performance. Figure 13 compares the tracking of the interceptor for a 2g pull-up and a 2g push-down by the target that started at radar lock on. In the 2g push-down maneuver the interceptor rolls onto its back and pulls down on the target. Also figure 13 shows that this large rolling maneuver causes little or no difference in the tracking performance of the interceptor.

SUMMARY OF RESULTS

With the use of an automatic interceptor system in which gravity considerations were omitted in the roll-command computation, the functioning of the error filter system with cross roll, the command computer, and the g-limiter have been studied. The two target conditions studied were a straight-flying target and a target that made a ±2g vertical-plane maneuver. The results of the investigation showed the following:

1. The inclusion of the cross-roll correction when filtering in a rotating axes system is desirable. This correction tends to reduce rolling accelerations and the amplitude of the rolling velocities which determine, to a large degree, the side forces acting on the pilot's head and the roughness of the motion experienced by the pilot.

2. The method used to compute the flight-path command proved satisfactory. However, the roll-command computation deteriorated as the smoothed elevation steering error approached zero. The two methods tried for the correction of this difficulty were only partially successful; how-

ever, the trends shown in these results appear to indicate that a satisfactory method of determining roll commands when gravity considerations are omitted from the command computation can be developed.

3. For the conditions of this study, the command type of g-limiter proved more satisfactory than the feedback type of g-limiter. The results obtained indicate that the operation of the command type of g-limiter is better when the longitudinal control system contains an inner-loop integrator than when the integrator is omitted.

4. The high-gain longitudinal control system provided acceptable tracking against targets performing ±2g vertical-plane maneuvers; however, the total error was beginning to approach unacceptable magnitudes.

5. The high-gain longitudinal control system and the g-limiter present conflicting requirements. The response of the former is better without the inner-loop integrator while the latter requires the inner-loop integrator in order to obtain an accurate normal acceleration restriction.

Langley Aeronautical Laboratory,
National Advisory Committee for Aeronautics,
Langley Field, Va., July 16, 1957.

1. Sherman, Windsor L., and Schy, Albert A.: Theoretical Investigation of the Attack Phase of an Automatic Interceptor System at Supersonic Speeds With Particular Attention to Aerodynamic and Dynamic Representation of the Interceptor. NACA RM L56J08, 1957.

2. Schy, Albert A., and Gates, Ordway B., Jr.: Analysis of Effects of Airplane Characteristics and Autopilot Parameters on a Roll-Command System With Aileron Rate and Deflection Limiting. NACA RM L55E18, 1955.

3. Woodling, C. H., and Gates, Ordway B., Jr.: Theoretical Analysis of the Longitudinal Behavior of an Automatically Controlled Supersonic Interceptor During the Attack Phase Against Maneuvering and Nonmaneuvering Targets. NACA RM L55G18, 1955.

4. Margolis, Kenneth, and Bobbitt, Percy J.: Theoretical Calculations of the Stability Derivatives at Supersonic Speeds for a High-Speed Airplane Configuration. NACA RM L53G17, 1953.

5. Anon.: Integrated Fire Control - Flight Control System IIN. Interim Engineering Rep. EM-185-7 (Contract No. NOas-52-222-C), North American Aviation, Inc., July 1, 1952, pp. 23-41.

6. Schy, Albert A., Gates, Ordway B., Jr., Woodling, C. H., Sherman, Windsor L., and Sternfield, Leonard: Simulator Studies of the Attack Phase of an Automatically Controlled Interceptor. I - Preliminary Studies of the Lateral and Longitudinal Control Systems, by Schy, Gates, and Woodling. II - Some Results of a Study Performed on the Typhoon Computer, by Sherman and Sternfield. NACA RM L55E27a, 1955.

TABLE I

INITIAL CONDITIONS FOR THE ATTACK PROBLEM

All angles in radians, all distances in feet, all velocities in feet per second or radians per second

Angle rotation order: Euler angles ψ, θ, ϕ reference space
Gimbal angles θ_a, θ_e reference body

Initial condition	I	II	III	IV	V
ψ_o	$-\frac{\pi}{2}$	$-\frac{\pi}{2}$	0	0	0
θ_o	0.0332	0.0332	0.0332	0.0332	0.0332
ϕ_o	0	0	0	0	0
V_{F_o}	2136	2136	2136	2136	2136
u_o	2135	2135	2135	2135	2135
v_o	0	0	0	0	0
w_o	70.52	70.52	70.52	70.52	70.52
R_o	60,000	60,000	60,000	60,000	60,000
θ_{a_o}	-0.08275	-0.1745	-0.7854	-0.7854	-0.2618
θ_{e_o}	0	0.1745	0	0.2618	0.2618
p,q,r	All zero initially				
V_T	1359 for all initial conditions $V_I = i(0) + j(1359) + h(0)$ in space				
H_T	50,000 for all initial conditions				
Speed of sound	971 for all initial conditions				

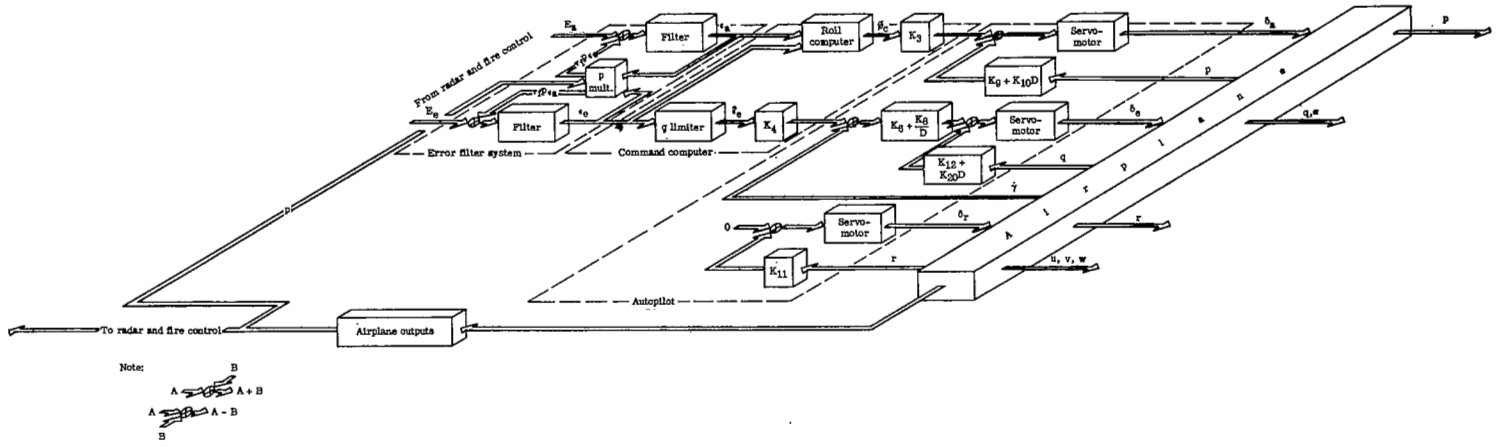

Figure 1.- Block diagram of interceptor flight-control system.

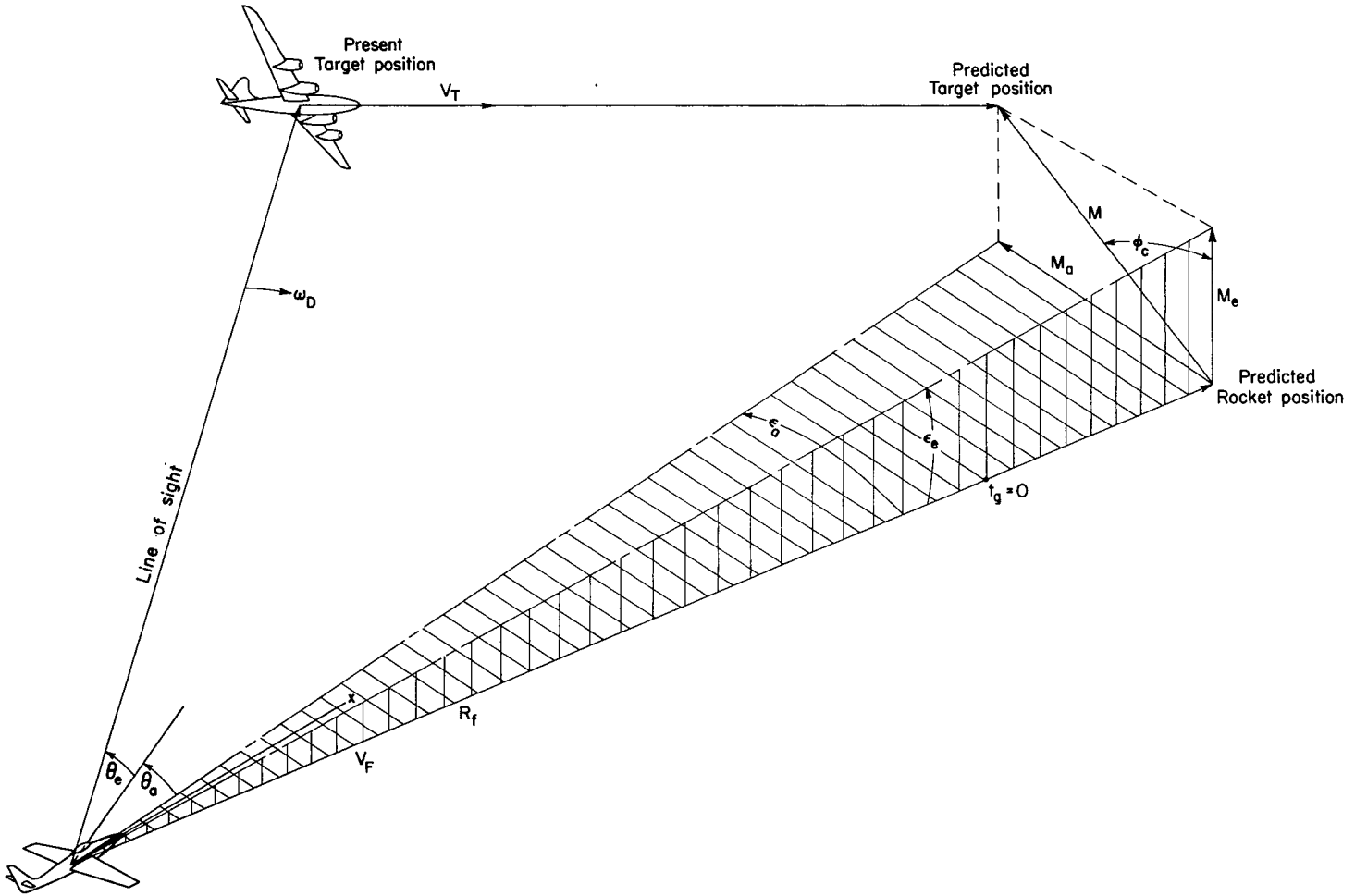

(a) Geometry of attack problem.

Figure 2.- Initial conditions.

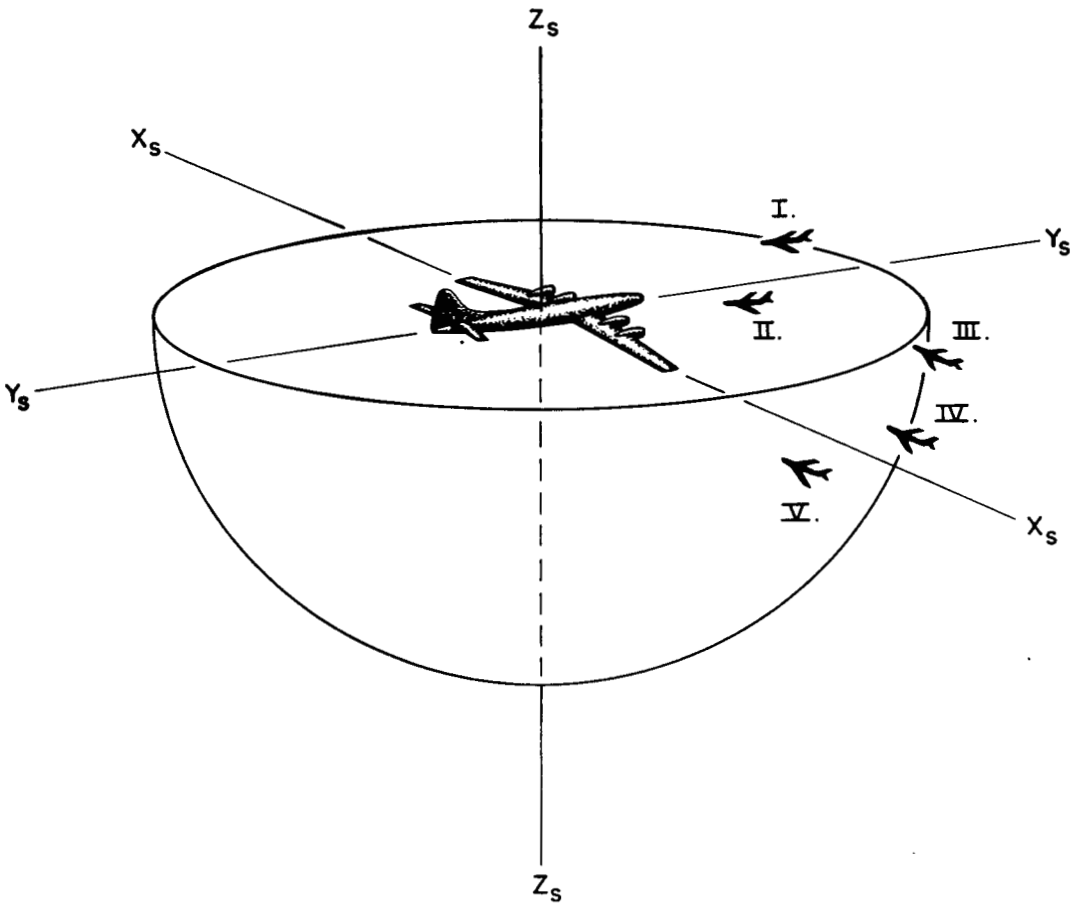

(b) Pictorial presentation of initial conditions.

Figure 2.- Concluded.

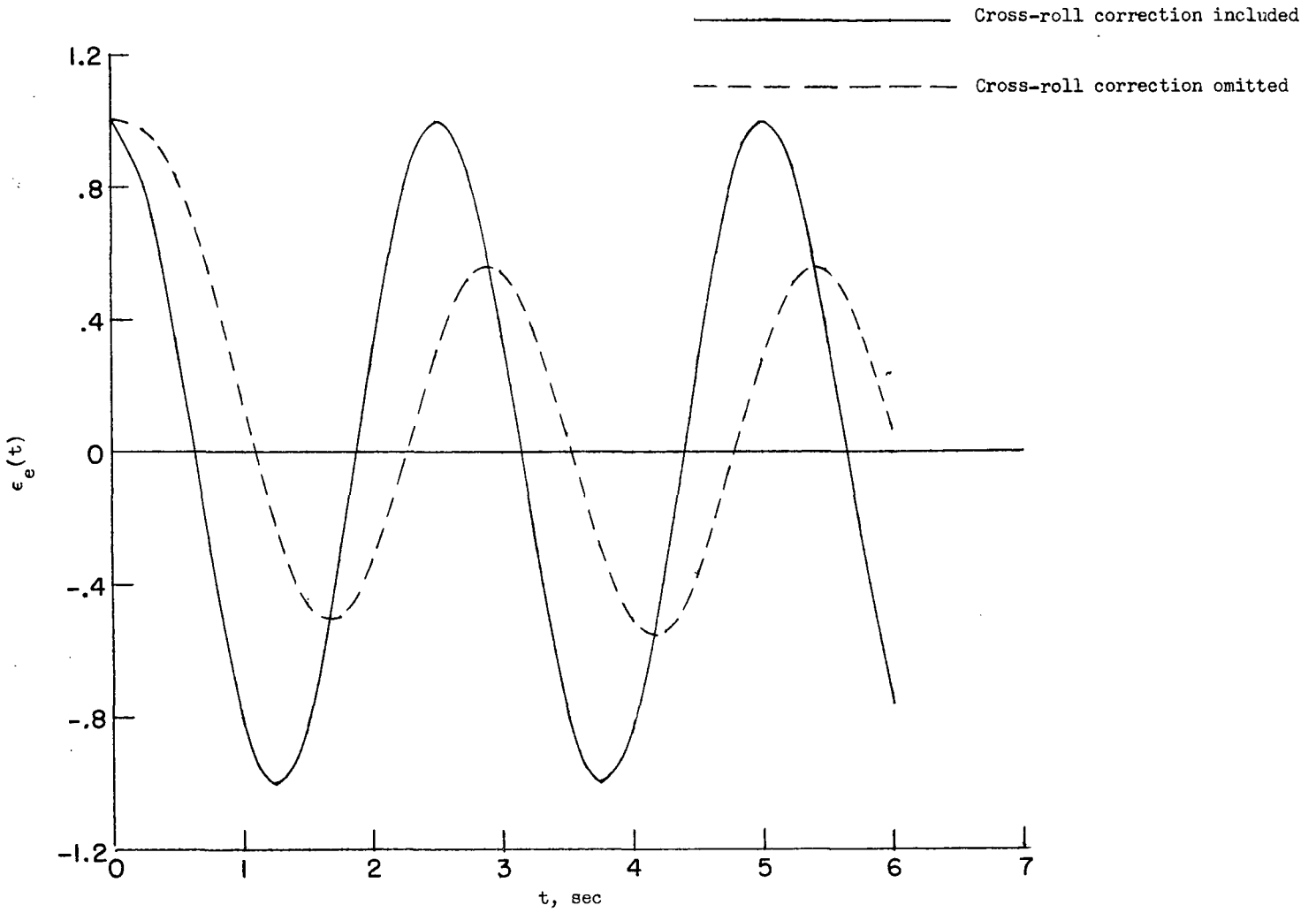

Figure 3.- Response of longitudinal channel of filter to sinusoidal input.

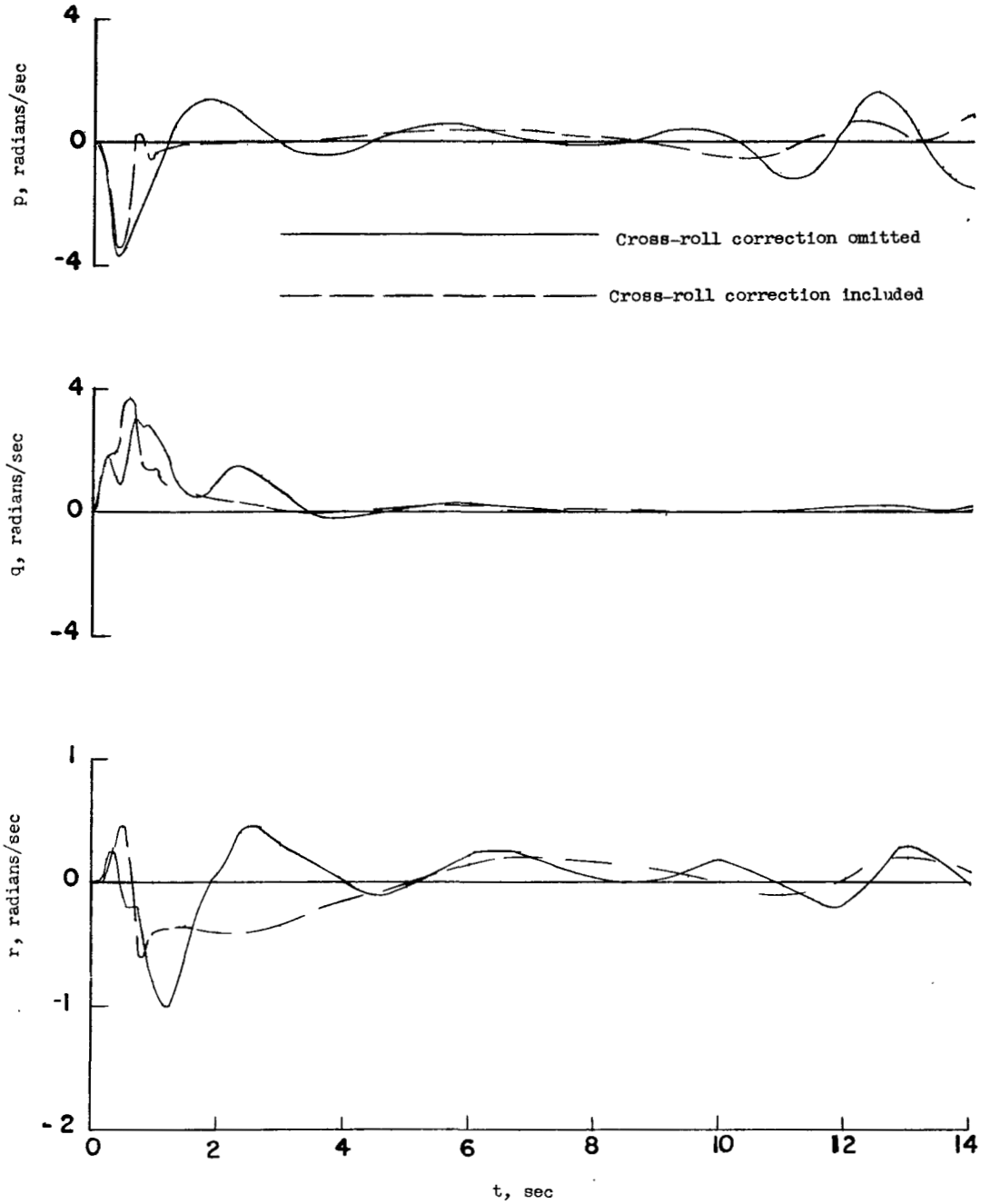

(a) Angular velocities.

Figure 4.- Comparison of airplane response with and without cross-roll correction included in filter. Initial condition I.

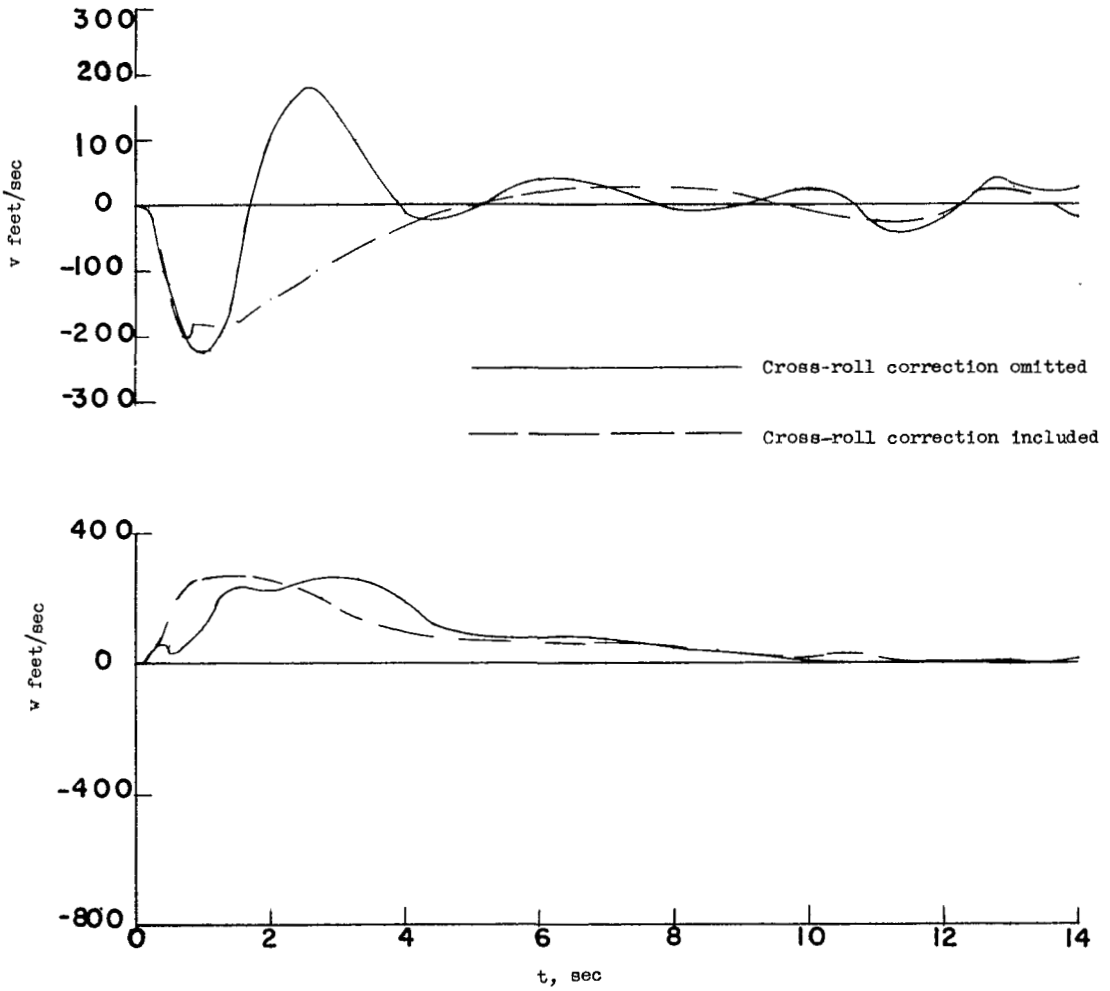

(b) Linear velocities.

Figure 4.- Concluded.

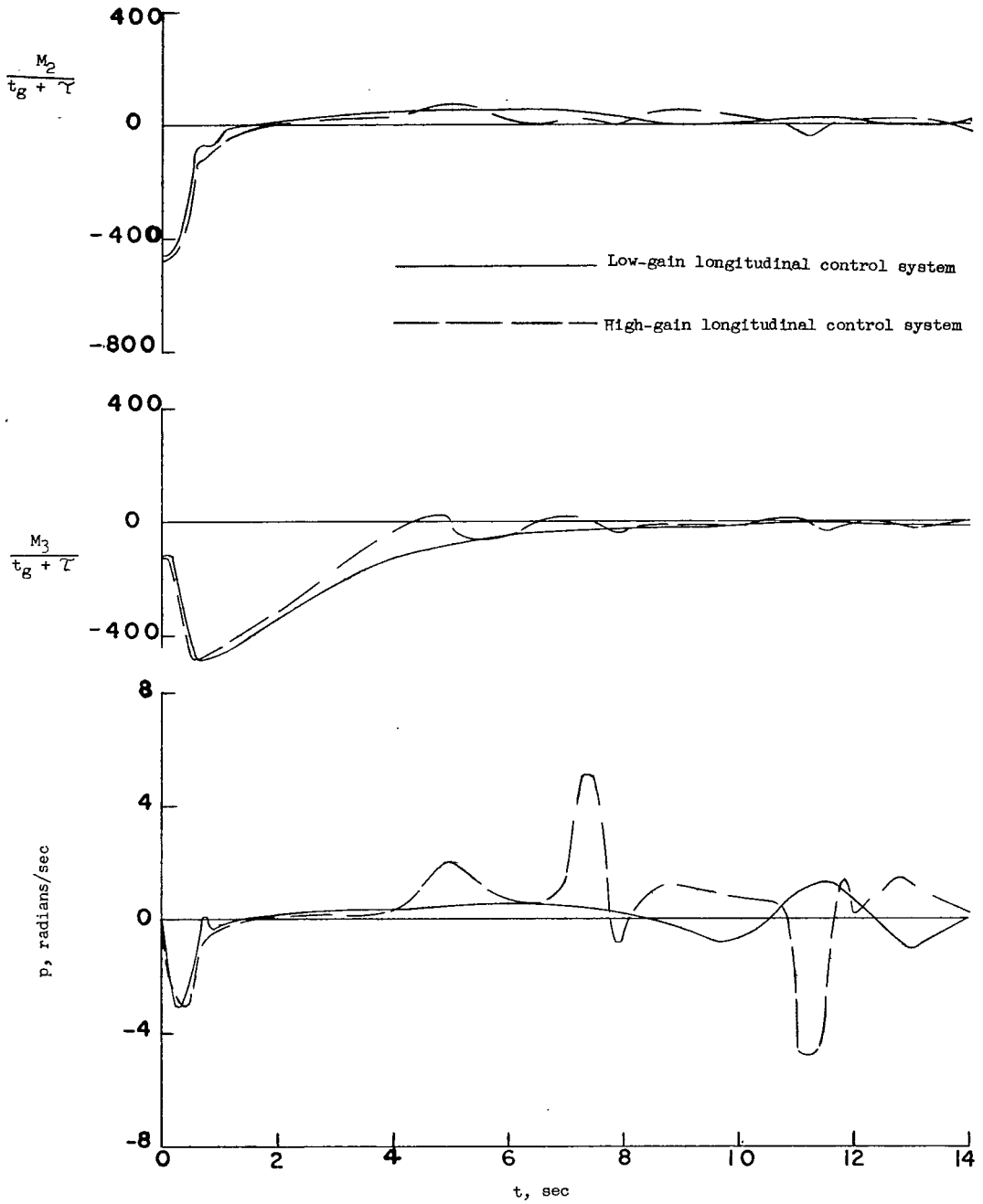

Figure 5.- Comparison of behavior of miss distance parameters $(M_2/t_g + \tau)$ and $(M_3/t_g + \tau)$ and roll response of the airplane for low-gain and high-gain longitudinal control systems. Initial condition I.

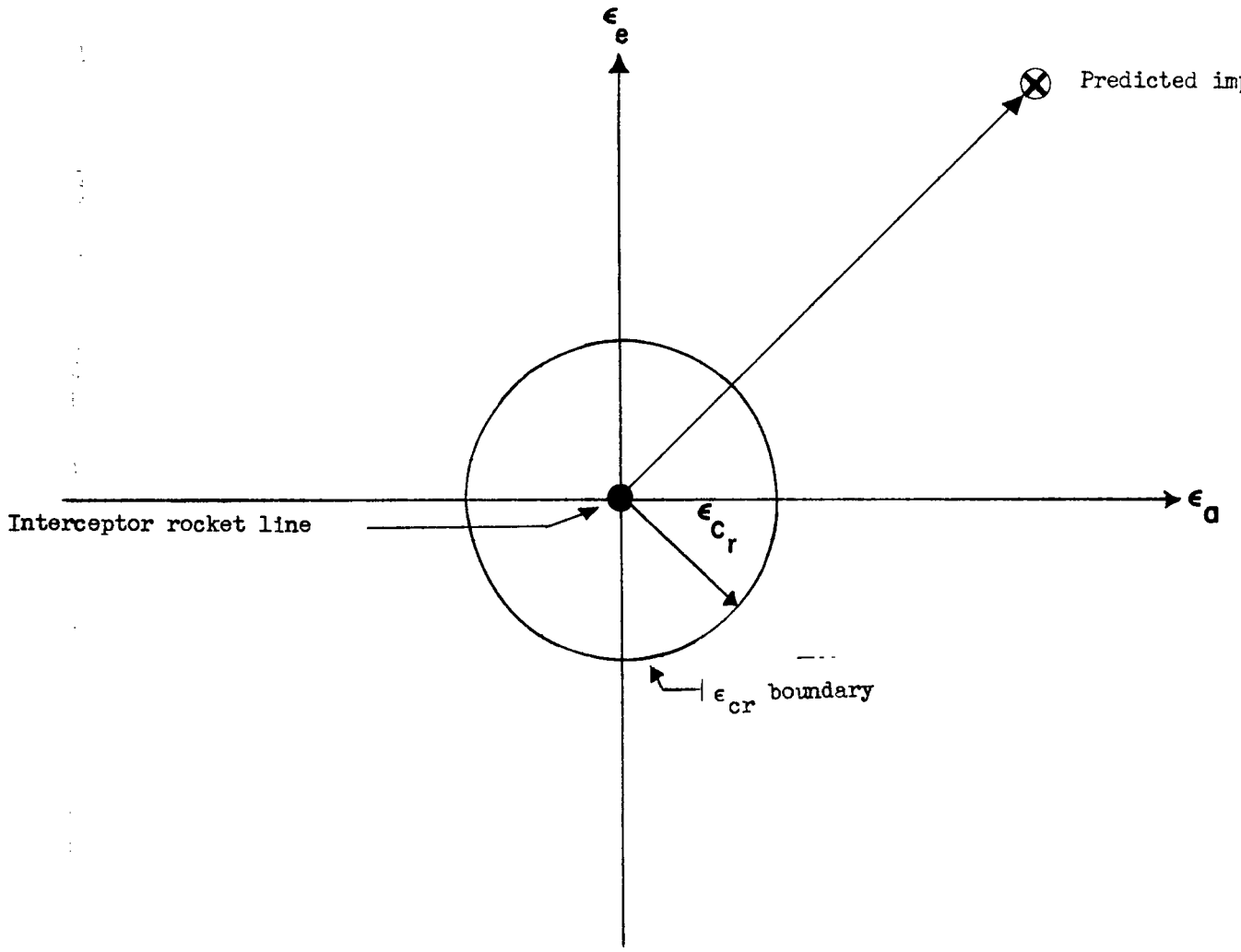

Figure 6.- Sketch showing relation of parameters for roll-command computation changes.

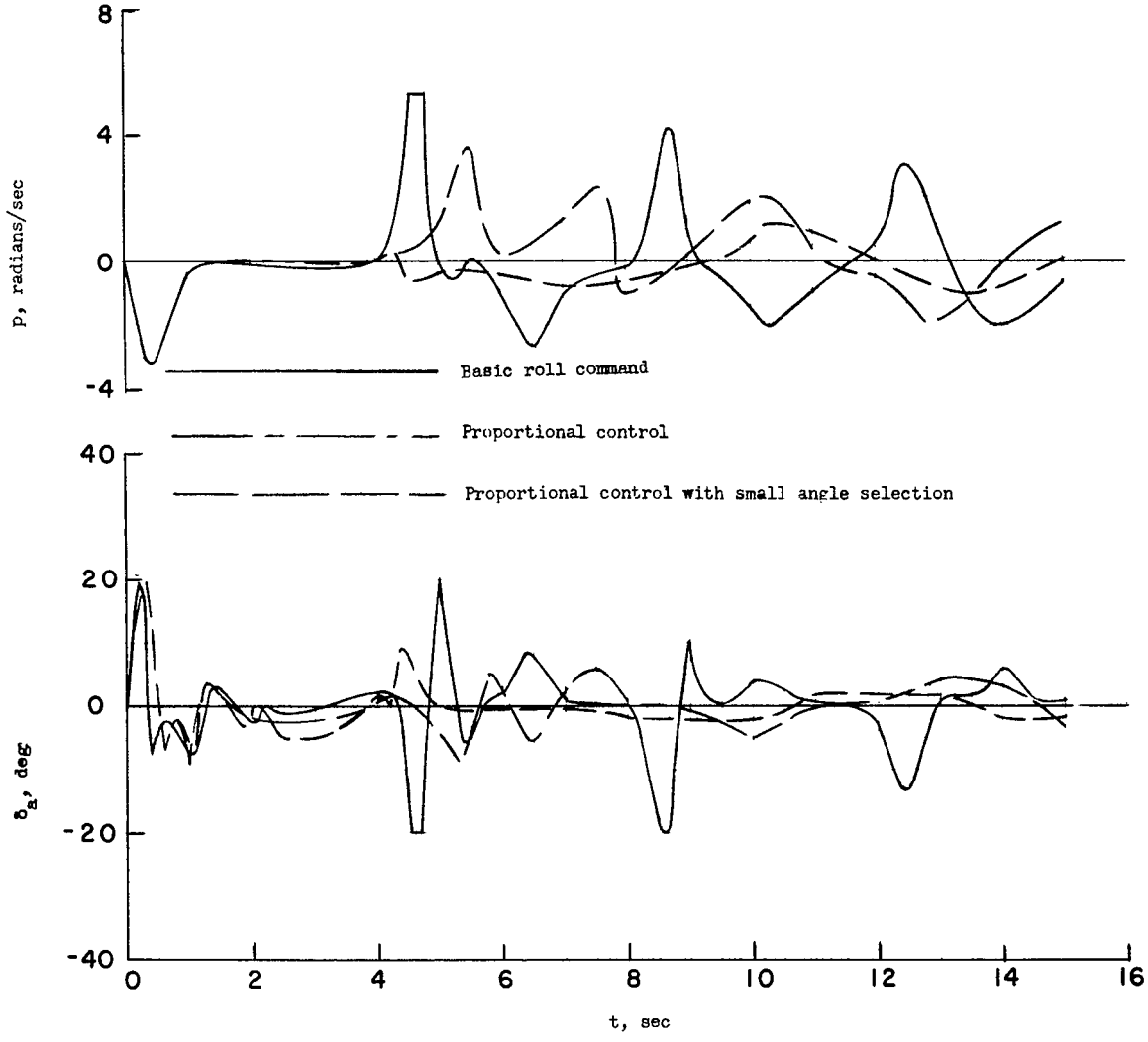

Figure 7.- Comparison of aileron and rolling responses for three different roll commands. Initial condition I; $\alpha_{cr} = 3^{\circ}$.

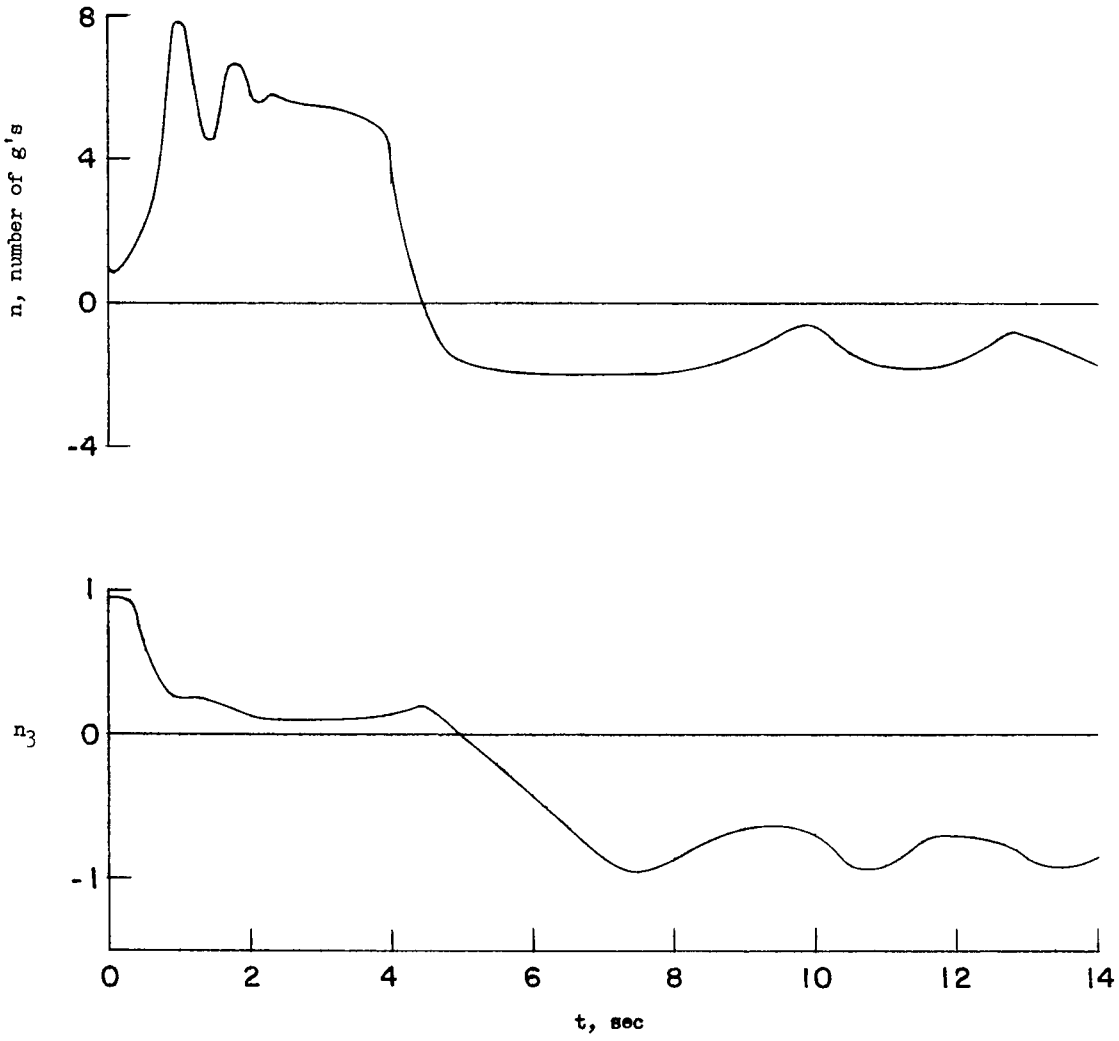

Figure 8.- Time histories of normal acceleration n and direction cosine n_3 obtained for a proportional roll command with small bank selection. Initial condition I.

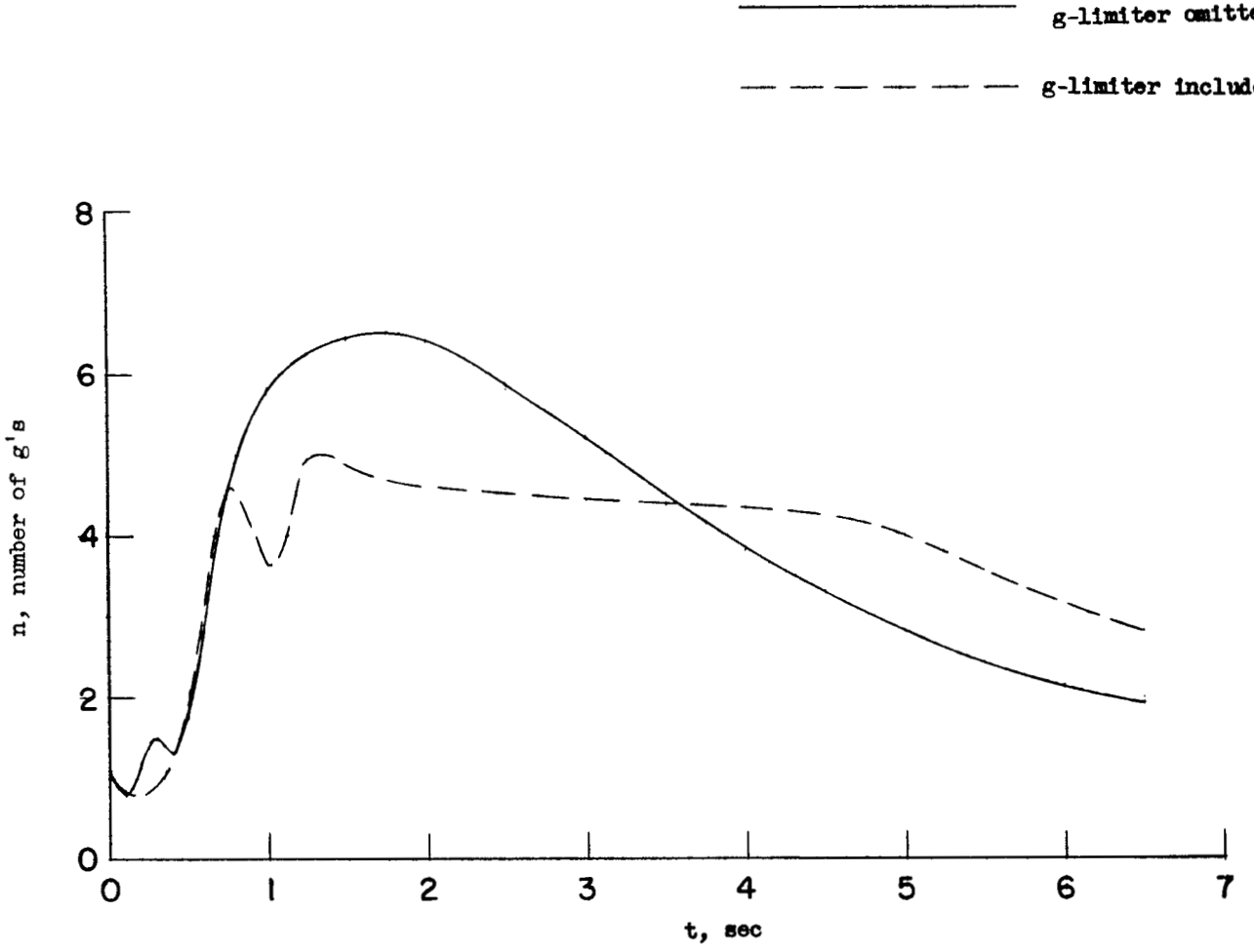

(a) Linear pitching-moment coefficient.

Figure 9.- Comparison of normal-acceleration response with and without a g-limiter and an inner-loop integrator in the longitudinal control system. Initial condition III.

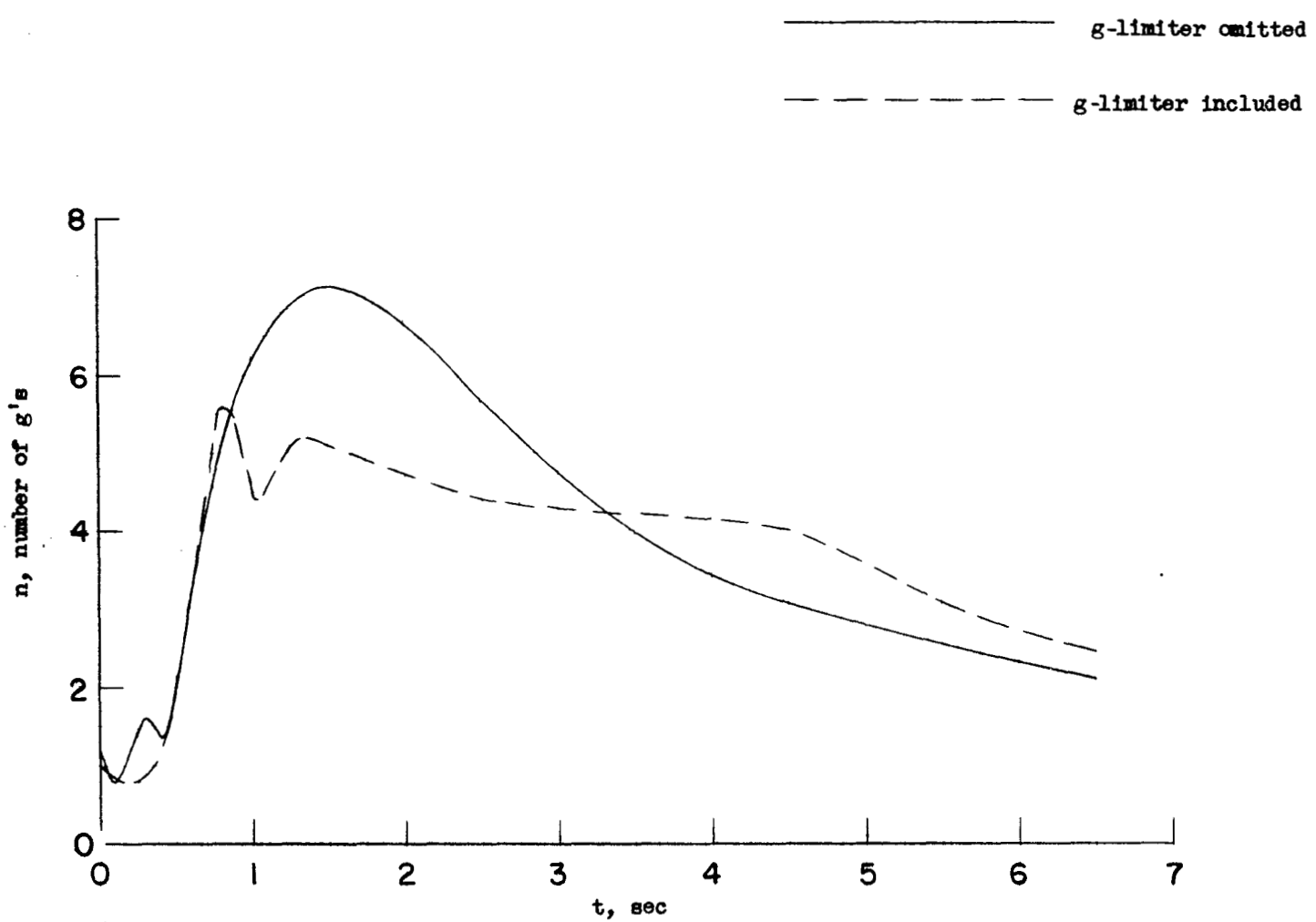

(b) Nonlinear pitching-moment coefficient.

Figure 9.- Concluded.

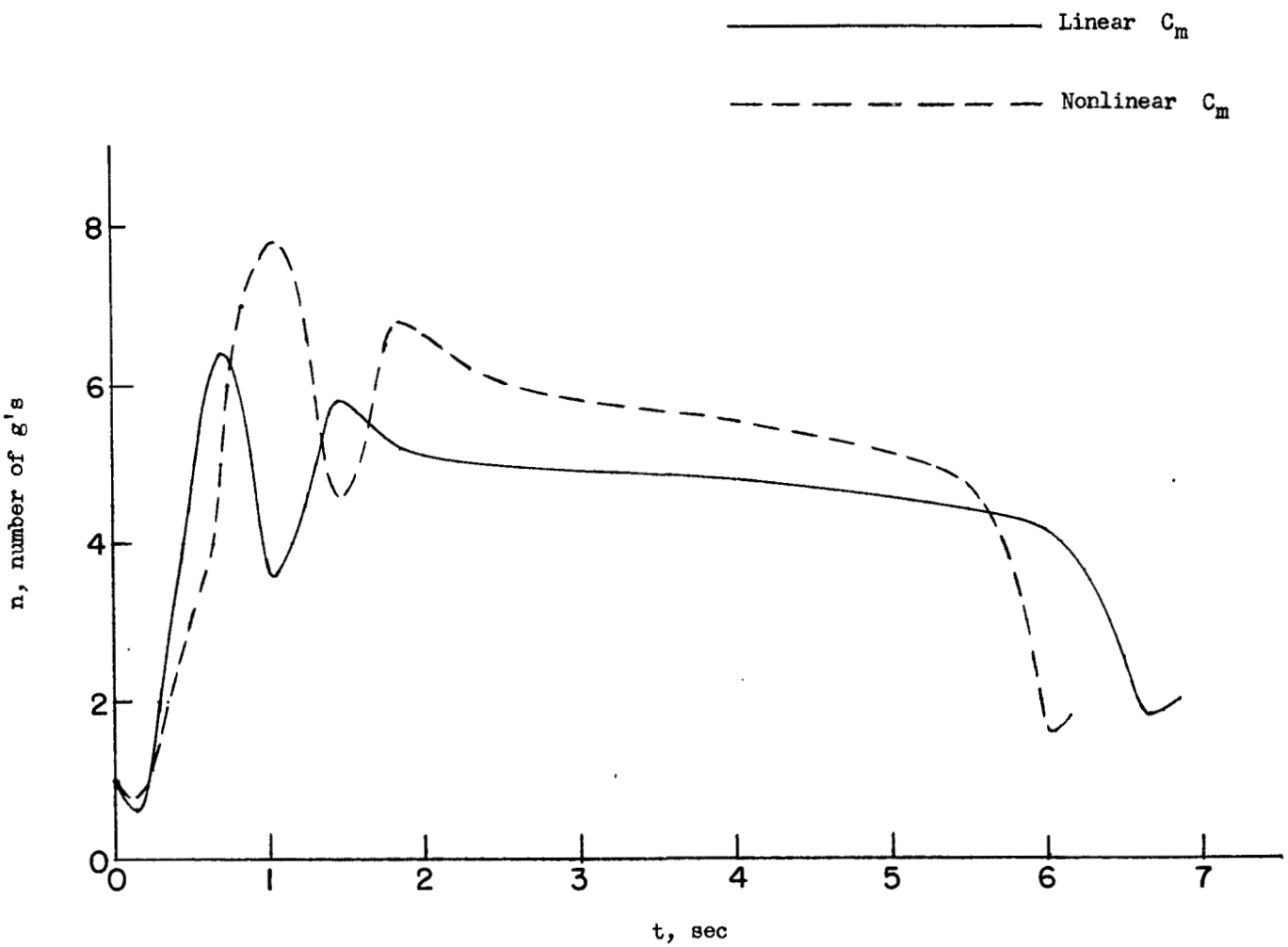

Figure 10.- Normal acceleration response of airplane with a command g-limiter and no inner-loop integrator in the longitudinal control system for linear and nonlinear pitching moments. Initial condition III.

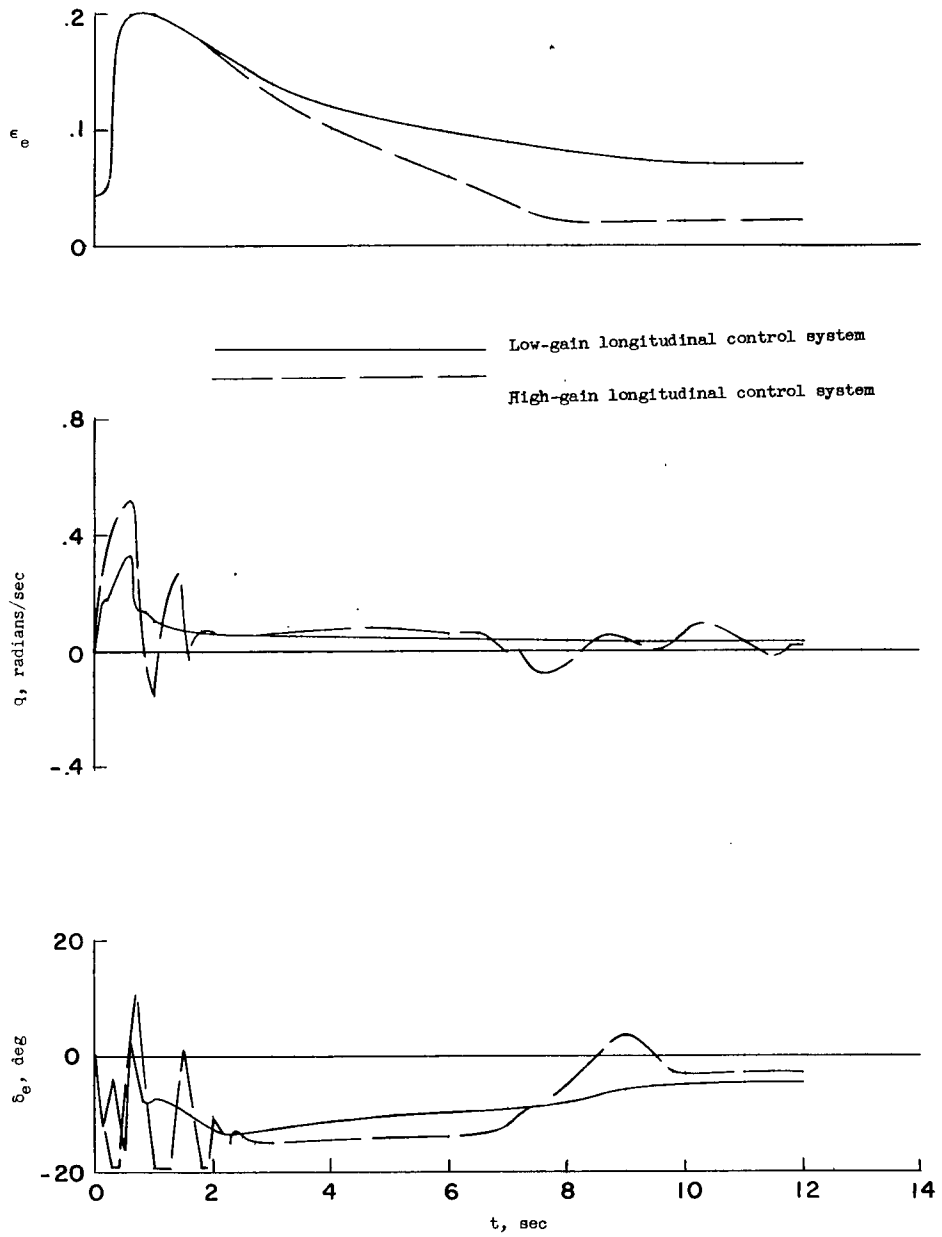

(a) Steering error ϵ_e, pitching velocity q, and elevator deflection δ_e.

Figure 11.- Comparison of longitudinal tracking ability of low-gain and high-gain longitudinal control systems target 2g vertical-plane maneuver. Attack run defined by initial condition I.

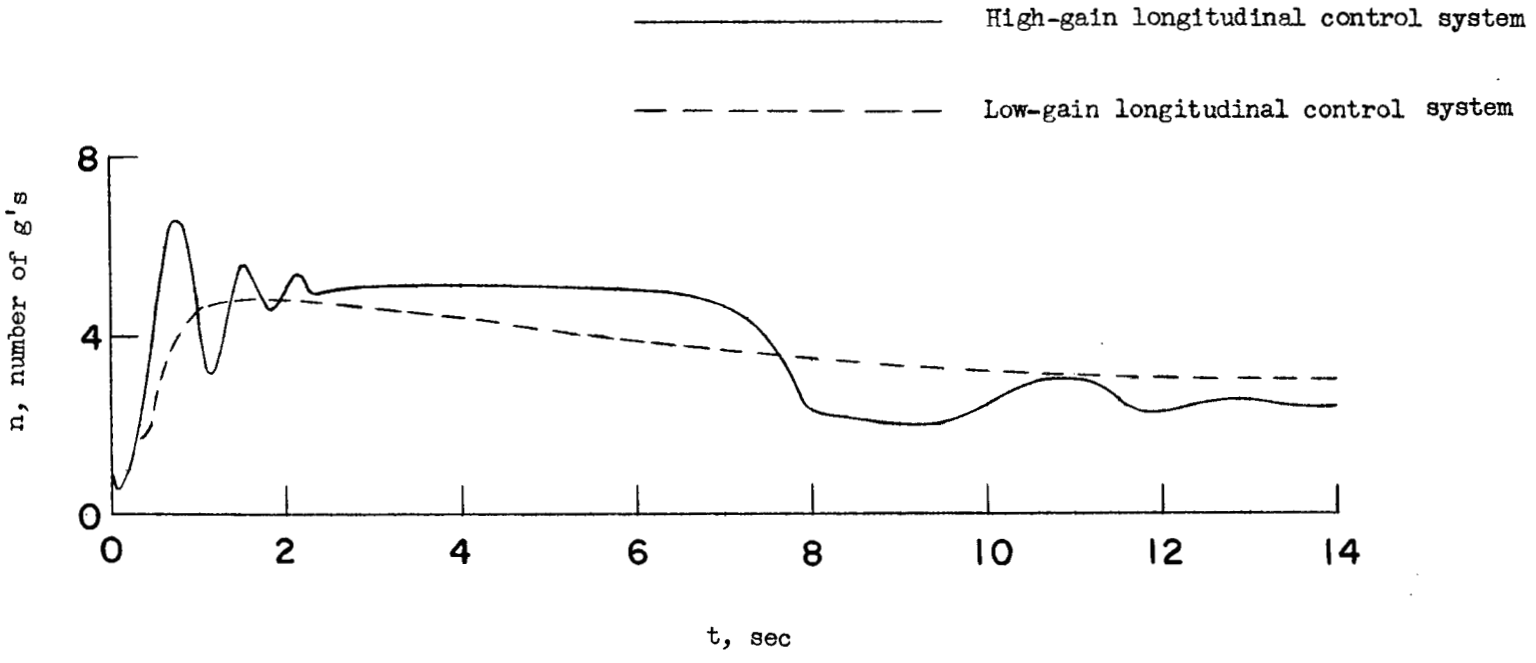

(b) Normal acceleration response.

Figure 11.- Concluded.

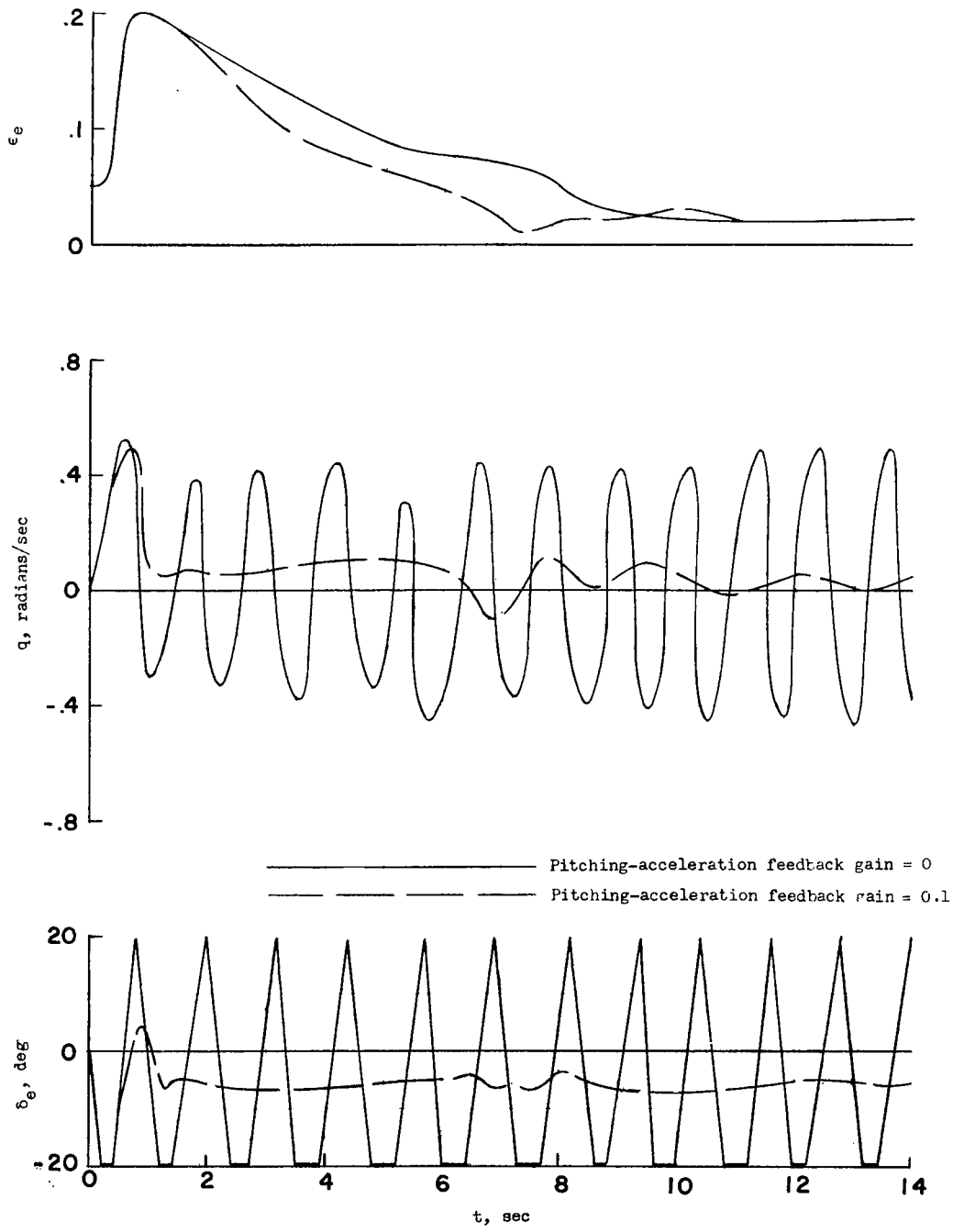

Figure 12.- Effect of pitching-acceleration feedback on longitudinal tracking performance. Target 2g vertical-plane maneuver. Interceptor initial condition I; nonlinear aerodynamics; $\alpha_{cr} = 6^{\circ}$.

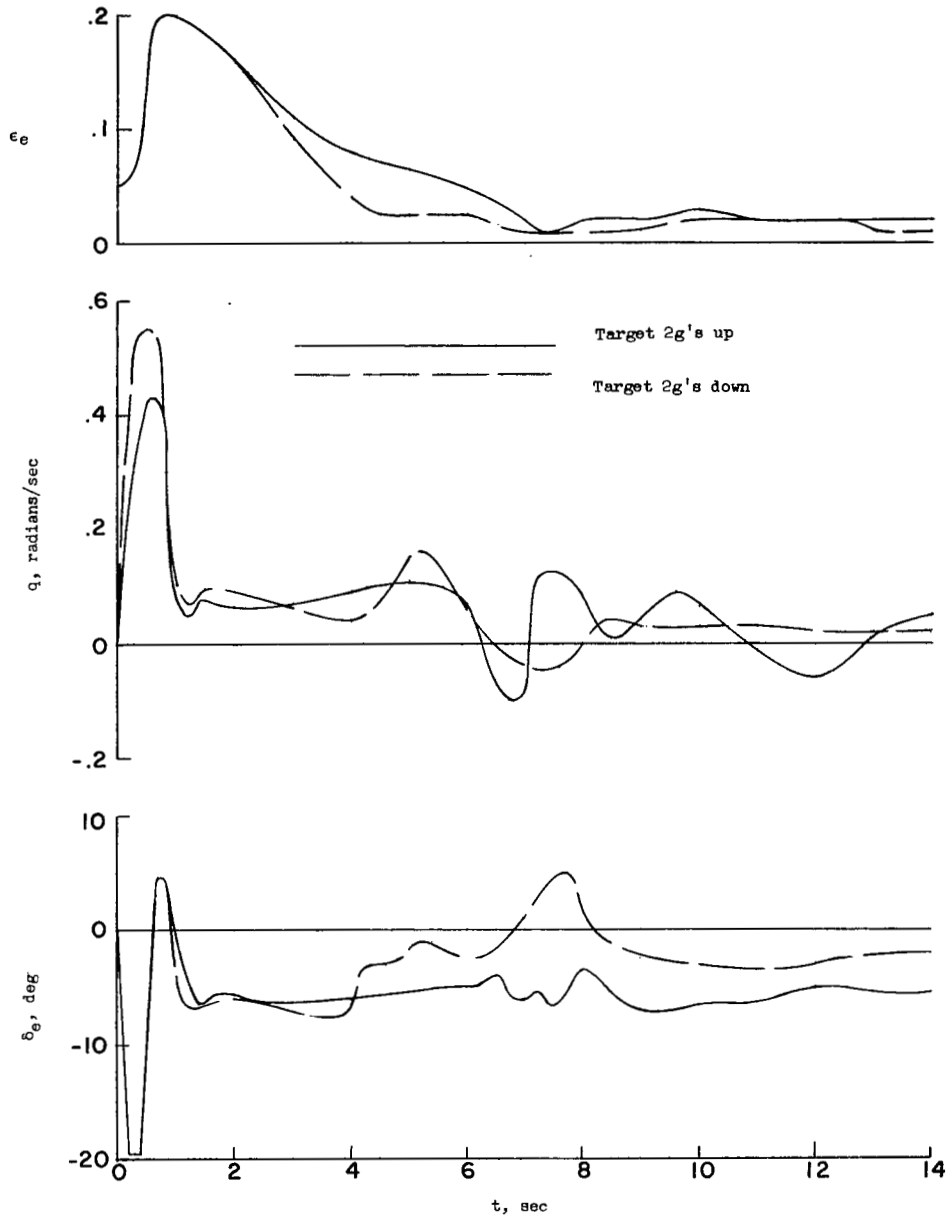

(a) Steering error ϵ_e, pitching velocity q, and elevator deflection δ_e.

Figure 13.- Comparison of longitudinal tracking performance for a 2g and a -2g vertical-plane target maneuver. High-gain longitudinal control system; initial condition I; aerodynamics varies with Mach number and angle of attack; $\alpha_{cr} = 6^\circ$.

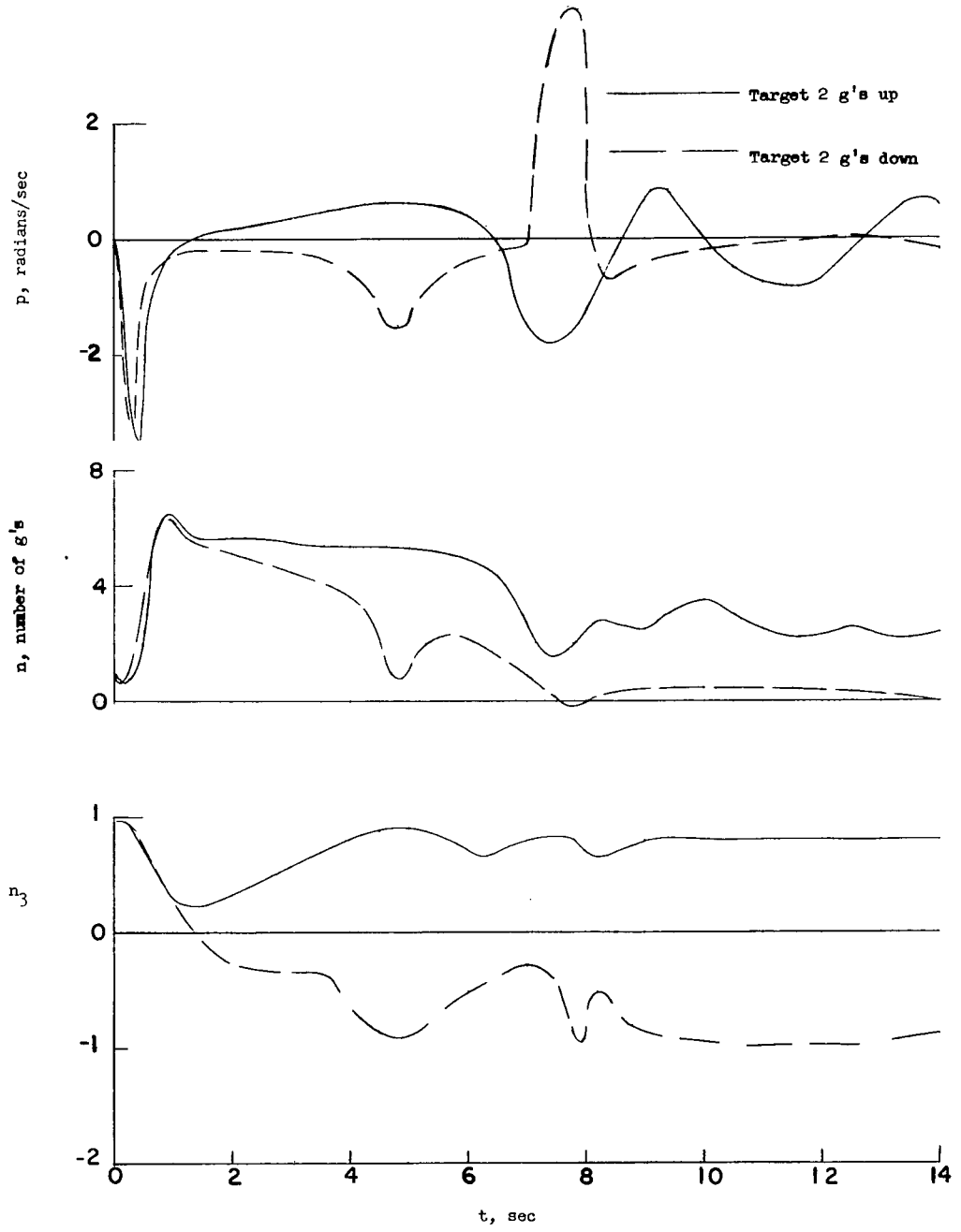

(b) Rolling velocity p, normal acceleration n, and direction cosine n_3.

Figure 13.- Concluded.